

# Model-independent determinations of the electron EDM and the role of diamagnetic atoms

Timo Fleig\*

*Laboratoire de Chimie et Physique Quantiques,  
IRSAMC, Université Paul Sabatier Toulouse III,  
118 Route de Narbonne, F-31062 Toulouse, France*

Martin Jung†

*Excellence Cluster Universe  
Technische Universität München  
Boltzmannstr. 2, D-85748 Garching, Germany*

## Abstract

We perform model-independent analyses extracting limits for the electric dipole moment of the electron and the P,T-odd scalar-pseudoscalar (S-PS) nucleon-electron coupling from the most recent measurements with atoms and molecules. The analysis using paramagnetic systems, only, is improved substantially by the inclusion of the recent measurement on  $\text{HfF}^+$  ions, but complicated by the fact that the corresponding constraints are largely aligned, owing to a general relation between the coefficients for the two contributions. Since this same relation does not hold in diamagnetic systems, it is possible to find atoms that provide essentially orthogonal constraints to those from paramagnetic ones. However, the coefficients are suppressed in closed-shell systems and enhancements of P,T-odd effects are only prevalent in the presence of hyperfine interactions. We formulate the hyperfine-induced time-reversal-symmetry breaking S-PS nucleon-electron interaction in general atoms in a mixed perturbative and variational approach, based on electronic Dirac-wavefunctions including the effects of electron correlations. The method is applied to the Hg atom, yielding the first direct calculation of the coefficient of the S-PS nucleon-electron coupling in a diamagnetic system. This results in additionally improved model-independent limits for both the electron EDM and the nucleon-electron coupling from the global fit. Finally we employ this fit to provide indirect limits for several paramagnetic systems under investigation.

---

\* timo.fleig@irsamc.ups-tlse.fr

† martin.jung@tum.de

## I. INTRODUCTION

Electric dipole moments (EDMs) provide a competitive means to search for new physics (NP), complementary to strategies like direct searches at hadron colliders, but also to other indirect searches, for instance using flavour-changing processes. The exceptional sensitivity is due to the combination of experimental precision with a tiny Standard Model (SM) background.<sup>1</sup> Experimental tests for EDMs involve typically rather complex systems like atoms or molecules. The discovery of a finite EDM in any of these systems would be a major discovery, independent of its specific source. However, reliably interpreting these measurements in terms of fundamental parameters of a given NP model requires precise knowledge of their relations. These are established proceeding via a series of effective field theories, rendering a large part of the analysis model- and system-independent, see *e.g.* Refs. [1–7] for recent reviews. The corresponding complex matrix elements on the atomic, nuclear and QCD levels often involve large uncertainties, which sometimes prohibit to fully exploit the experimental information, see Refs. [5, 8] for recent detailed discussions.

This article presents a new method for the rigorous calculation of the coefficient of the scalar-pseudoscalar nucleon-electron (S-PS-ne) interaction in diamagnetic systems. For this contribution so far only rough estimates exist, due to the fact that it vanishes to leading order in the electromagnetic interaction, even in the presence of an external electric field. In this paper we consider Mercury (Hg) which provides the strongest experimental limit on an EDM so far [9]. The determination of this coefficient provides a competitive limit on the (NP-induced) strength of the corresponding interaction. It is also of special interest for the model-independent extraction of the electron EDM: in principle, paramagnetic systems can be used to obtain both coefficients, taking into account potential cancellations [10, 11]; however, a problem arises from the fact that all paramagnetic systems constrain a similar combination of these two contributions [10]. Diamagnetic systems generally give independent constraints, thereby improving the model-independent extraction of both coefficients significantly [11]. Our results can therefore be used to constrain different classes of NP models, requiring less restrictive assumptions.

This article proceeds as follows: In the following section we present a method for the direct calculation of S-PS-ne enhancements in closed-shell atoms and molecules. Section III describes its application to the Hg atom, and in section IV we investigate the phenomenological consequences of the present study. In the final section we conclude and discuss the implications of our findings for future work.

---

<sup>1</sup> *Strong CP violation* constitutes a potential exception to this statement; however, the neutron EDM indicates a tiny value for this contribution as well.

## II. THEORETICAL FRAMEWORK

The calculation of the dominant contribution induced by the S-PS-ne interaction in diamagnetic systems requires the inclusion of the hyperfine interaction on top of the corresponding calculation in paramagnetic systems, since its expectation value vanishes to leading order in a closed-shell atom, due to a vanishing spin density near its nucleus [12, 13]. The nuclear current at the origin, corresponding to the magnetic moment of the nucleus, polarizes the closed atomic shells and leads to non-zero values. In a traditional setup this would require a three-fold expansion in the S-PS-ne interaction, the external electric field and the hyperfine interaction. Instead, we here start from a 0th-order electronic-structure problem

$$\hat{H}^{(0)} \left| \psi_K^{(0)} \right\rangle = \varepsilon_K^{(0)} \left| \psi_K^{(0)} \right\rangle, \quad (1)$$

where  $H^{(0)}$  is the atomic Dirac-Coulomb Hamiltonian *including* the perturbation due to a homogeneous external electric field  $\mathbf{E}_{\text{ext}}$ , with the nucleus placed at the origin:

$$\begin{aligned} \hat{H}^{(0)} &:= \hat{H}^{\text{Dirac-Coulomb}} + \hat{H}^{\text{Int-Dipole}} \\ &= \sum_j^N \left[ c \boldsymbol{\alpha}_j \cdot \mathbf{p}_j + \beta_j c^2 + \frac{Z}{r_j} \mathbb{1}_4 \right] + \sum_{j,k>j}^N \frac{1}{r_{jk}} \mathbb{1}_4 + \sum_j \mathbf{r}_j \cdot \mathbf{E}_{\text{ext}} \mathbb{1}_4, \end{aligned} \quad (2)$$

where the indices  $j, k$  run over  $N$  electrons,  $Z$  is the proton number ( $N = Z$  for neutral atoms), and  $\boldsymbol{\alpha}, \beta$  are standard Dirac matrices. We use atomic units (*a.u.*) throughout ( $e = m_0 = \hbar = 1$ ). Since we solve Eq. (1) variationally (*i.e.*, by diagonalization), the effect of the external electric field in  $\left| \psi_K^{(0)} \right\rangle$  is taken into account to all orders in perturbation theory. These states are technically electronic configuration interaction (CI) vectors [14].

The first-order perturbed wavefunction due to the magnetic hyperfine interaction can be written as

$$\left| \psi_J^{(1)} \right\rangle = \left| \psi_J^{(0)} \right\rangle + \sum_{K \neq J} \frac{\langle \psi_K^{(0)} | \hat{H}_{\text{HF}}^{(1)} | \psi_J^{(0)} \rangle}{\varepsilon_J^{(0)} - \varepsilon_K^{(0)}} \left| \psi_K^{(0)} \right\rangle, \quad (3)$$

where in practice the summation is carried out over a restricted set of CI vectors. The perturbation sum in Eq. (3) will only be well-defined if  $\left| \psi_J^{(0)} \right\rangle$  is a non-degenerate state, which is the case for the electronic ground state of a closed-shell atom.

Since  $\hat{H}_{\text{HF}}^{(1)}$  is a totally symmetric operator with respect to all valid symmetry operations of the system including the external field (axial symmetry), the sum in Eq. (3) includes only states of the same irreducible representation as the reference

state  $|\psi_J^{(0)}\rangle$ . The magnetic hyperfine Hamiltonian reads

$$\hat{H}_{\text{HF}} = -\frac{1}{2c m_p} \frac{\mu \mathbf{I}}{I} \cdot \sum_{i=1}^n \frac{\boldsymbol{\alpha}_i \times \mathbf{r}_i}{r_i^3}, \quad (4)$$

where  $\mu = gI$  is the nuclear magnetic moment,  $g$  the nuclear  $g$ -factor,  $m_p$  the proton mass and  $\mathbf{I}$  the nuclear spin. The minus sign in Eq. (4) relates to the charge of an electron in *a.u.* The hyperfine Hamiltonian can also be written as  $\hat{H}_{\text{HF}}^{(1)} = \mathbf{I} \mathcal{A} \mathbf{J}$ , where  $\mathcal{A}$  is the rank 2 cartesian hyperfine interaction tensor and  $\mathbf{J}$  is the total electronic angular momentum. It is, therefore, generally a sum of nine terms that due to  $\mu := \langle I, M_I = I | \hat{\mu}_z | I, M_I = I \rangle$  and  $\boldsymbol{\mu} \propto \mathbf{I}$  reduces to  $\hat{H}_{\text{HF}}^{(1)} = I_z (\mathcal{A}_{zx} J_x + \mathcal{A}_{zy} J_y + \mathcal{A}_{zz} J_z)$ . The required matrix elements are defined as follows:

$$(A_{zk})_{MN} = -\frac{\mu[\mu_N]}{2c I m_p} \sum_{i=1}^n \left\langle \psi_M^{(0)} \left| \left( \frac{\boldsymbol{\alpha}_i \times \mathbf{r}_i}{r_i^3} \right)_k \right| \psi_N^{(0)} \right\rangle, \quad (5)$$

where  $k$  is a cartesian component and the nuclear magnetic moment enters in units of the nuclear magneton  $\mu_N = \frac{1}{2cm_p}$  (in *a.u.*).

For evaluating the S-PS-ne enhancement in the atom we use the effective Hamiltonian operator [15]

$$\hat{H}_{\text{S-PS-ne}}^{(1)}(S) = i \frac{G_F}{\sqrt{2}} A C_S \sum_e \gamma_e^0 \gamma_e^5 \rho(\mathbf{r}_e), \quad (6)$$

where  $G_F$  is the Fermi constant,  $A$  the nucleon number,  $C_S$  the dimensionless S-PS-ne coupling constant,  $\rho$  the normalized nuclear charge density, and  $\gamma^\mu$  are standard Dirac matrices. Given the smallness of this interaction, even compared to the hyperfine interaction, higher-order perturbative corrections are clearly negligible. Given, furthermore, the CP-conserving nature of the hyperfine interaction, the energy shift of a given atomic state indicating CP violation can to leading order be written as

$$(\Delta\varepsilon)_J = \frac{1}{\langle \psi_J^{(1)} | \psi_J^{(1)} \rangle} \left\langle \hat{H}_{\text{S-PS-ne}}^{(1)} \right\rangle_{\psi_J^{(1)}}. \quad (7)$$

The atomic EDM in terms of the S-PS-ne interaction is a function of the polarizing external electric field  $E_{\text{ext}}$ , and so

$$d_a = - \lim_{E_{\text{ext}} \rightarrow 0} \left[ \frac{\partial(\Delta\varepsilon)}{\partial E_{\text{ext}}} \right] \approx -A C_S \frac{G_F}{\sqrt{2}} \frac{\left\langle i \sum_e \gamma_e^0 \gamma_e^5 \rho(\mathbf{r}_e) \right\rangle_{\psi^{(1)}(E_{\text{ext}})}}{E_{\text{ext}} \langle \psi^{(1)} | \psi^{(1)} \rangle} \equiv \alpha_{C_S} C_S, \quad (8)$$

where the approximation holds in the linear regime which is assured by external fields chosen significantly smaller than the internal ones and we have introduced  $\alpha_{C_S}$ , the

atomic S-PS-ne enhancement factor. In the present case  $E_{\text{ext}}(\text{Hg}) = 0.00024 \text{ a.u.}$ . This leads to shifts of the energies  $\varepsilon_K^{(0)}$  (see Eq. (1)) on the order of  $10^{-6} \text{ a.u.}$  for Hg. CI vectors are consequently optimized such that the energies  $\varepsilon_K^{(0)}$  are converged to at least  $10^{-9} \text{ a.u.}$

We now focus on the evaluation of the normalized expectation value, part of the expression on the right-hand side of Eq. (8),

$$\begin{aligned} & \frac{1}{\langle \psi_J^{(1)} | \psi_J^{(1)} \rangle} \left\langle \psi_J^{(1)} \left| i \sum_e \gamma_e^0 \gamma_e^5 \rho(\mathbf{r}_e) \right| \psi_J^{(1)} \right\rangle = \\ & \frac{1}{\langle \psi_J^{(1)} | \psi_J^{(1)} \rangle} \left[ \sum_{K \neq J} \frac{\langle \psi_K^{(0)} | \hat{H}_{\text{HF}}^{(1)} | \psi_J^{(0)} \rangle}{\varepsilon_J^{(0)} - \varepsilon_K^{(0)}} \left\langle \psi_J^{(0)} \left| i \sum_e \gamma_e^0 \gamma_e^5 \rho(\mathbf{r}_e) \right| \psi_K^{(0)} \right\rangle \right. \\ & \quad \left. + \sum_{K \neq J} \frac{\langle \psi_J^{(0)} | \hat{H}_{\text{HF}}^{(1)} | \psi_K^{(0)} \rangle}{\varepsilon_J^{(0)} - \varepsilon_K^{(0)}} \left\langle \psi_K^{(0)} \left| i \sum_e \gamma_e^0 \gamma_e^5 \rho(\mathbf{r}_e) \right| \psi_J^{(0)} \right\rangle \right], \end{aligned} \quad (9)$$

up to higher-order terms in the hyperfine interaction, where we used the hyperfine-perturbed wavefunction from Eq. (3). The leading term in this equation (for open-shell atoms) vanishes for closed-shell atoms, and is omitted. This conclusion has also been tested numerically in the present work. Transition matrix elements of the type  $\langle \psi_K^{(0)} | \hat{H}_{\text{HF}}^{(1)} | \psi_J^{(0)} \rangle$  and  $\langle \psi_K^{(0)} | i \sum_e \gamma_e^0 \gamma_e^5 \rho(\mathbf{r}_e) | \psi_J^{(0)} \rangle$ , required for evaluating these two terms, can be readily made available using the developed methodology in Refs. [16, 17]. The practical problem is then to provide a sufficient set of CI states for the perturbation sum. The final expression for evaluating the S-PS-ne enhancement is, therefore,

$$\alpha_{C_S}(\psi_J) = \frac{-A \frac{G_F}{\sqrt{2}}}{E_{\text{ext}} \langle \psi_J^{(1)} | \psi_J^{(1)} \rangle} \left[ \sum_{K \neq J} \frac{\langle \psi_K^{(0)} | \hat{H}_{\text{HF}}^{(1)} | \psi_J^{(0)} \rangle}{\varepsilon_J^{(0)} - \varepsilon_K^{(0)}} \left\langle \psi_J^{(0)} \left| i \sum_e \gamma_e^0 \gamma_e^5 \rho(\mathbf{r}_e) \right| \psi_K^{(0)} \right\rangle + h.c. \right] \quad (10)$$

For convenience, we use in the following also the S-PS-ne enhancement  $S$  (in analogy to the electron EDM enhancement  $R$  and not to be confused with the nuclear Schiff moment, also denoted  $S$  in the literature), defined as

$$S := \frac{d_a}{A C_S \frac{G_F}{\sqrt{2}}} = \frac{\alpha_{C_S}}{A \frac{G_F}{\sqrt{2}}} \approx - \frac{\left\langle i \sum_e \gamma_e^0 \gamma_e^5 \rho(\mathbf{r}_e) \right\rangle_{\psi^{(1)}(E_{\text{ext}})}}{E_{\text{ext}} \langle \psi^{(1)} | \psi^{(1)} \rangle}. \quad (11)$$

In order to facilitate comparison with the literature, we note that the states  $|\psi_K^{(0)}\rangle$  can be considered as wavefunctions perturbed to infinite order by  $\mathbf{E}$ , and so

the expression in Eq. (9) contains terms of third order of the type

$$\sum_{K,N \neq J} \frac{\langle \psi_J^{(0)} | \sum_i \hat{r}_z(i) | \psi_N^{(0)} \rangle E_z \langle \psi_K^{(0)} | \hat{H}_{\text{HF}}^{(1)} | \psi_J^{(0)} \rangle}{\left( \varepsilon_J^{(0)} - \varepsilon_N^{(0)} \right) \left( \varepsilon_J^{(0)} - \varepsilon_K^{(0)} \right)} \langle \psi_N^{(0)} | \imath \sum_e \gamma_e^0 \gamma_e^5 \rho(\mathbf{r}_e) | \psi_K^{(0)} \rangle, \quad (12)$$

plus higher-order contributions in  $\mathbf{E}$ , where  $|\psi_N^{(0)}\rangle$  is now an unperturbed eigenstate of the plain atomic Dirac-Coulomb Hamiltonian *without* external electric field. The terms in Eq. (12) are just the equivalent of the electron EDM contribution via magnetic hyperfine interaction to an atomic EDM, as given by Flambaum and Khriplovich in reference [15], Eq. (17). These third-order terms, declared important but left untreated in reference [18], are taken into account in the present approach. Moreover, the higher-order contributions in  $\mathbf{E}$  are included automatically in the present approach.

### III. NE-SPS ENHANCEMENT IN ATOMIC MERCURY

For our zeroth-order atomic wavefunctions the quantum number  $M_J$ , corresponding to the projection of the total angular momentum onto the axis defined by the external electric field, is an exact quantum number and characterizes an irreducible representation of the axial double point group. Since the external perturbation is small, the quantum number  $J$  is still approximately valid and we denote CI states in the approximate Russell-Saunders picture as  $^M L_{J,M_J}$ , where  $M$  is the spin multiplicity. The S-PS-ne interaction Hamiltonian in Eq. (6) is rotationally invariant; as a consequence,  $\langle M_J | \hat{H}_{\text{S-PS-ne}} | M'_J \rangle = 0$  for  $M_J \neq M'_J$ , which reduces the perturbation sum in Eq. (9) to states from the irreducible representation  $M_J = 0$ , a computational advantage which we exploit.

Applying the framework developed in the last section to Mercury, a consistent finding in all our calculations is that among the 35 energetically lowest-lying excited states of symmetry  $M_J = 0$  only three states contribute sizably to the perturbation sum Eq. (9) determining  $\alpha_{CS}$ , namely  $\psi_K^{(0)} \in \{^3 P_{0,M_J=0}(5d^{10}6s6p), ^3 S_{1,M_J=0}(5d^{10}6s7s), ^3 P_{0,M_J=0}(5d^{10}6s7p)\}$ . This finding can be understood qualitatively analyzing the product of matrix elements in Eq. (9): For contributions of the type

$$\langle ^3 P_{0,M_J=0} | \hat{H}_{\text{HF}}^{(1)} | ^1 S_{0,M_J=0} \rangle \langle ^1 S_{0,M_J=0} | \imath \sum_e \gamma_e^0 \gamma_e^5 \rho(\mathbf{r}_e) | ^3 P_{0,M_J=0} \rangle$$

the off-diagonal S-PS-ne matrix element is large due to the parity-odd excitation  $6s \rightarrow np$  characterizing the excited state, and the off-diagonal hyperfine matrix element is non-negligible due to  $sp$ -mixing *via* the external electric field. For the

other leading type of contribution,

$$\langle {}^3S_{1,M_J=0} | \hat{H}_{\text{HF}}^{(1)} | {}^1S_{0,M_J=0} \rangle \langle {}^1S_{0,M_J=0} | \sum_e \gamma_e^0 \gamma_e^5 \rho(\mathbf{r}_e) | {}^3S_{1,M_J=0} \rangle,$$

the off-diagonal S-PS-ne matrix element is now two orders of magnitude smaller than in the above case – for obvious reasons related to symmetry –, but the off-diagonal hyperfine matrix element becomes almost three orders of magnitude larger than for the previous mechanism. This is explained by the fact that the excited state  ${}^3S_1$  exhibits a non-vanishing spin-density near the nucleus.

Results from many-body models of different sophistication are compiled in Table I. The S-PS-ne enhancement is largely converged when at least the 12 lowest-lying  $M_J = 0$  states are included in the perturbation sum, since then the three main contributors are covered.

Basis/cutoff	# of CI states $M_J = 0$ /Model/X	Meandev. %	$\frac{S}{10^{-2} a.u.}$	$\frac{\alpha_{C_S}}{10^{-22} ecm}$
DZ/150 a.u.	4/M12/6p7s7p6d5f8p8s7d		-3.3	-5.4
DZ/150 a.u.	16/M12/6p7s7p6d5f8p8s7d		-2.3	-3.8
TZ/50 a.u.	12/M12/6p7s7p	6.1	-2.1	-3.5
TZ/50 a.u.	12/M20/6p7s7p		-2.1	-3.5
TZ/50 a.u.	12/M12/6p7s7p6d8p8s	5.4	-2.2	-3.7
TZ/50 a.u.	29/M12/6p7s7p6d8p8s9p9s10p10s	6.2	-2.22	-3.67

TABLE I. S-PS-ne interaction ratio  $S$  for the  ${}^1S_0$  ground state of the  ${}^{199}\text{Hg}$  isotope,  $I = 1/2$ ,  $\mu({}^{199}\text{Hg}) = +0.5058855$  [19],  $E_{\text{Ext}} = 0.00024$  a.u.; CI models M12: 12 electrons correlated, Single, Double and Triple excitations from occupied space into X, Single and Double excitations into the remaining virtual space (SDT12-X-SD12); M20: S8-SDT12-X-SD20. DZ and TZ denote Dyal’s Gaussian atomic basis sets [20, 21] including 1f,1g valence- and core-correlating exponents (DZ) and 2f,4g,1h valence- and core-correlating and valence-polarizing exponents (TZ), resulting in a total of 24s,19p,12d,8f,1g for DZ and 30s,24p,15d,11f,4g,1h functions for TZ. The mean deviation concerns the difference of the calculated excited-state energies from experiment [22]. The Hg nucleus is described by a Gaussian charge distribution [23] with exponent  $\zeta = 1.4011788914 \times 10^8$ .

It is furthermore important that the extent of the active spinor space is sufficient, as can be seen from the results for different values of  $X$ , the parameter defining the atomic functions constituting the space into which triple excitations are allowed. The remaining virtual spinors up to the cutoff threshold are allowed to be up to doubly occupied, in order to include dynamic electron correlation effects for all states described to lowest order by the structure of the active space. Correlation effects between 5s, 5p and valence electrons are tested through the model including 20 electrons and are seen to be small.

For the purpose of estimating the contribution from higher-lying excited states we use a larger basis set, denoted QZ and consisting of 34s,30p,19d,13f,4g,2h functions. Due to computational demand the model M12 is limited to X-SDT12 with X set to the value 7p7s8p9p8s10p9s with reference to Table I. This means that correlation effects are largely neglected for a large set of small contributions,  $\approx 100$  states with  $M_J = 0$ . We observe that only two notable contributions occur, and only in the energetically lower half, indicating that the contributions as expected fall off as energy and principal quantum number of the involved states increase. With the resulting enhancement correction  $\Delta S(\text{QZ})$ , where  $S$  is defined in Eq. (11), our final value is obtained as follows:

$$S(\text{TZ}) + \Delta S(\text{QZ}) = (-2.22 + 0.53) \times 10^{-2} a.u. = -1.69 \times 10^{-2} a.u. \quad (13)$$

The uncertainty of this value is estimated by *linearly* adding the errors from the energy denominator (6.2%, “mean deviation” in Table I), and uncertainties from atomic basis set (3.5%), outer-core correlations (1.5%), and higher excitation ranks (5%, estimated from comparable previous calculations of S-PS-ne enhancements, see Refs. [24, 25]). To this uncertainty of 16% on the base value  $S(\text{TZ})$  we add an uncertainty of 30% times the relative weight (0.24) of the correction  $\Delta S(\text{QZ})$ , *i.e.*, 7.2%, resulting in a total uncertainty of 23% for  $\alpha_{C_S}$ , which we consider very conservative. Note that adding the individual terms in quadrature, as commonly done in the literature, would result in an uncertainty of 11%. From these considerations, we finally obtain from Eq. (13) the S-PS-ne interaction constant

$$\alpha_{C_S} = -2.8(6) \times 10^{-22} e \text{ cm} . \quad (14)$$

An indirect determination of  $\alpha_{C_S}$  is obtained *via* the coefficient of the (P,T)-odd tensor interaction, using the phenomenological relation [13, 15, 26]

$$\frac{\langle \boldsymbol{\sigma} \rangle \cdot \mathbf{I}}{I} \alpha_{C_S} = 5.3 \times 10^{-4} (1 + 0.3 Z^2 \alpha^2) A^{2/3} \mu_A \alpha_{C_T} , \quad (15)$$

where  $\langle \boldsymbol{\sigma} \rangle_{C_T} \equiv \langle \sum_{N=n,p} C_T^N \boldsymbol{\sigma}_N \rangle$  ( $\langle \dots \rangle$  denoting the expectation value over a nuclear state with spin  $\mathbf{I}$ ),  $\mu_A$  denotes the magnetic moment of the atom’s nucleus (in units of the nuclear magneton), and the coefficients  $C_T^N$  parametrize the tensorial (P,T)-odd electron-nucleon interaction,

$$\mathcal{H}_T = \frac{iG_F}{\sqrt{2}} \sum_{N=n,p} C_T^N (\bar{N} \boldsymbol{\sigma}_{\mu\nu} \gamma_5 N) (\bar{e} \boldsymbol{\sigma}_{\mu\nu} e) . \quad (16)$$

To further facilitate the comparison with other works, we note that the coefficient of the tensor interaction is typically parametrized *via*  $\mathbf{d}_A = 10^{-20} C_{C_T} \langle \boldsymbol{\sigma} \rangle_{C_T} e \text{ cm}$ , implying

$$\alpha_{C_T} = 10^{-20} C_{C_T} \frac{\langle \boldsymbol{\sigma} \rangle \cdot \mathbf{I}}{I} e \text{ cm} . \quad (17)$$



Method	Ref.	$C_{C_T}$	$\alpha_{C_S}/(10^{-22} e \text{ cm})$
RPA	[27]	-6.0	(-6.0)
MCDHF	[28]	-4.8	(-4.8)
CI+MBPT	[18]	-5.1	(-5.1)
PRCC	[29]	-4.3	(-4.3)
CCSD <sup>(∞)</sup>	[30]	-3.4	(-3.4)
CCSD <sub>p</sub> T(+)	[31]	-4.0	(-4.0)
CCSD <sub>p</sub> T(+)	[32]	-3.2	(-3.2)
NCCSD	[33]	-3.3	(-3.3)
Chupp <i>et al.</i> (est.)	[7, 34]		(-5.9)
Engel <i>et al.</i> (est.)	[5]		(-8.1)
This work		(-2.8)	<b>-2.8</b>

TABLE II. Comparison of the direct calculation presented here with previous calculations of  $\alpha_{C_S}$ , using calculations of  $\alpha_{C_T}$  and the phenomenological relation Eq. (15) (indicated by parentheses around the result,  $\mu_{Hg} = 0.506$ ). The literature values are ordered as to increasing sophistication of the treatment of dynamic electron correlation. Numerically the conversion factor for Mercury reads  $\alpha_{C_S}^{\text{Hg}} = 10^{-2} \alpha_{C_T}^{\text{Hg}} / (\langle \boldsymbol{\sigma} \rangle \cdot \mathbf{I}/I)$ , and a simple shell model for the nucleus is used, yielding  $\langle \boldsymbol{\sigma} \rangle \cdot \mathbf{I}/I = -1/3$ .

The comparison is shown in Table II. We note that effects of interelectron correlations reduce  $C_{C_T}$  by about a factor of 1/2. Due to relations (15) and (17) these effects are expected to be qualitatively similar for the coefficient  $\alpha_{C_S}$ . In our result from the direct calculation electron correlation effects among the outermost 20 electrons of the Hg atom have been taken into consideration. There are two main sources for a potential difference between our value and the Coupled Cluster (CC) results *via* the phenomenological relation: 1) Our correlation model differs from the correlation models used in the CC calculations. 2) The phenomenological relation employs a uniform nuclear charge density whereas in our calculations a more realistic Gaussian charge distribution is used (see Table I) [35]. Since correlation effects tend to reduce the absolute value of  $\alpha_{C_S}$  and our value is already about 15% below the CC results, it is reasonable to assume that no major correlation effects have been missed in our final computational model. The present difference is furthermore within the expected precision of this relation.

#### IV. PHENOMENOLOGICAL CONSEQUENCES

In order to explore the phenomenological consequences of our results, we follow two different strategies: (i) The common method to limit the corresponding Wilson

coefficients assuming the absence of cancellations, *i.e.* setting all other contributions to zero. (ii) Limiting *both*  $C_S$  and the electron EDM  $d_e$  model-independently, *i.e.* allowing for cancellations between the two. This is achieved by combining information from the Mercury system with that of paramagnetic ones, following Ref. [11], using the experimental results in Table III. The key point in this strategy is that Mercury constrains a linear combination of  $d_e$  and  $C_S$  that is approximately orthogonal to the one constrained from paramagnetic systems, specifically ThO. This observation can be used to constrain  $C_S$  and  $d_e$ , following a three-step argument:

Molecule	$\omega_{\text{exp}}/(\text{mrad/s})$	Refs.
HfF <sup>+</sup>	$0.3 \pm 2.7 \pm 0.6^{\text{a}}$	[36]
ThO	$2.6 \pm 4.8 \pm 3.2$	[37, 38]
YbF	$5.3 \pm 12.6 \pm 3.8$	[39, 40]
Atom	$d_A/(e \text{ cm})$	Refs.
Tl	$-(4.0 \pm 4.3) \times 10^{-25}$	[41]
Hg	$(2.20 \pm 2.75 \pm 1.48) \times 10^{-30}$	[9]

<sup>a</sup> Adapted to match the conventions used here.

TABLE III. Experimental limits for the systems entering the global fit.

1. The EDMs of paramagnetic systems are to good approximation dominated by contributions from  $d_e$  and  $C_S$  [42–44].<sup>2</sup> While  $C_S$  depends in general on the system under consideration, the combination that enters heavy atoms and molecules is to good approximation universal [11].  $C_S$  cannot be neglected model-independently: while NP models exist where the electron EDM clearly gives the leading contribution, this is not true in general. In Two-Higgs-Doublet models (2HDMs) for instance, the dominating Barr-Zee diagram for the electron EDM avoids a second small mass factor in addition to  $m_e$ , but as a two-loop diagram competes with a tree contribution to the S-PS-ne coupling that is suppressed by a light-quark mass and contains additional small factors like gauge couplings [8]. Schematically, we have  $m_{u,d,s} \times \text{tree}$  vs.  $m_t \times \text{two-loop} \sim m_t/(16\pi^2)^2$ .
2. Both contributions can in principle easily be taken into account, once two experiments with comparable sensitivity are available. The problem is that

<sup>2</sup> Strictly speaking also contributions from the Schiff moment and in some cases the magnetic quadrupole moment of the nucleus in paramagnetic systems could cancel these enhanced contributions. Given the large enhancement of the latter by  $Z^3 \sim 10^5$ , this would however imply huge contributions in other systems, which are at least as severely constrained. However, formally a chain of cancellations in all constrained systems remains a possibility, due to the large number of potential sources.

most of the constraints from paramagnetic systems are essentially parallel, so that typically fine-tuned solutions exist, where electron EDM and S-PS-ne contributions *both* oversaturate the experimental limit, but cancel to large extent in the measured observables. This leads to a situation where the model-independent approach yields a limit on the electron EDM that is about a factor of 10 weaker than the naive limit obtained when setting the S-PS-ne coupling to zero. This situation can be resolved by measurements on systems with different slopes, for example with relatively light atoms like Rb and very heavy ones like Fr. The recent measurement [36] already improves the situation significantly, as shown below.

3. In diamagnetic systems, there are many contributions to a potential EDM; assuming the presence of only electron EDM and S-PS-ne contributions here is clearly not a good description of, e.g. , the Mercury EDM. However, the different hierarchy in this case can be used to turn the argument around: In diamagnetic systems both contributions are *not* enhanced, but strongly suppressed, because they yield a non-vanishing contribution only in combination with the hyperfine splitting. The sensitivity of Mercury to the electron EDM is about  $3 \times 10^8$  weaker than in ThO. The sensitivity to other contributions, like quark (C)EDMs, the theta term, and even tensor electron-nucleon couplings is much higher. This is why it is conservative to assume that these – often neglected – contributions saturate the experimental limit.

The conditions that have to be met for the resulting limit to be invalid are consequently very specific:

- The individual electron EDM and S-PS-ne contributions to the relevant paramagnetic systems would have to be larger than the experimental limits, but cancel in all of them sufficiently well.
- The electron EDM and S-PS-ne contributions to Hg would also have to be larger than the experimental limit, despite the massively different sensitivity.
- Since in the latter case a cancellation between the two contributions in Hg is not possible simultaneously with the paramagnetic systems, other contributions, that are each individually expected to be much larger than those from the electron EDM or S-PS-ne couplings, would have to combine in such a way that the net effect on the Hg EDM is again smaller than the experimental limit.

It is not impossible that all these things happen simultaneously, but since several cancellations on very different levels and in very different systems are necessary, we

consider the limit resulting from our procedure conservative. Assumptions are made only on a subleading level, while in the literature it is very common to make them at the leading level, *i.e.* simply neglecting the S-PS-ne coupling. For convenience we provide below also the results without this assumption, *i.e.* when using the data from paramagnetic systems, only.

Note that the calculation presented here will remain useful even if the procedure outlined above should become unnecessary because of measurements in paramagnetic systems providing sufficiently precise and non-parallel constraints. Ultimately the goal should be a global analysis separating as many sources for EDMs as possible, see Ref. [34] for a first attempt. Should both  $d_e$  and  $C_S$  be determined/limited from paramagnetic systems alone, the impact of the Mercury measurement on the remaining sources will increase, given a sufficiently precise determination of the corresponding coefficients.

Starting with strategy (i), *i.e.* assuming  $C_S$  to give the only contribution to the Mercury EDM, we obtain from Ref. [9] and Eq. (14)

$$C_S = - (0.8_{-1.2}^{+1.5}) \times 10^{-8}, \quad \text{or} \quad |C_S| \leq 3.2 \times 10^{-8} \text{ (95\% CL)} \quad (C_S \text{ only}). \quad (18)$$

This value is significantly larger than the one given in Ref. [9], for two reasons: Heckel et al. used an indirectly obtained value for  $\alpha_{C_S}$  [27], where moreover electron correlation effects have largely been neglected, which is much larger than our result on the absolute (and also larger than newer indirectly obtained results), and presumably used only the central value of that result. It is also significantly larger than the values obtained from ThO ( $|C_S| \leq 0.7 \times 10^{-8}$  (95% CL)) and HfF<sup>+</sup> ( $|C_S| \leq 1.8 \times 10^{-8}$  (95% CL)); However, as we will see below, the Hg result nevertheless improves the global fit significantly.

We perform global fits to the available data in Table III, using the theoretical inputs given in Table IV. The molecular measurements are typically expressed in terms of the angular frequency  $\omega_M$ , which can for our purposes be written as

$$\omega_M = \left( -1.52 \operatorname{sgn}(\Omega) \frac{E_{\text{eff}}}{\text{GV/cm}} \frac{d_e}{10^{-27} e \text{ cm}} + 2\pi \cdot 10^6 \Omega \frac{A_M}{Z_M} \frac{W_S}{\text{kHz}} C_S \right) \langle \hat{n} \cdot \hat{z} \rangle \frac{\text{mrad}}{\text{s}} \quad (19)$$

$$\equiv \alpha_{d_e}^M d_e + \alpha_{C_S}^M C_S, \quad (20)$$

where  $E_{\text{eff}}$  the effective electric field,  $\Omega = \langle \mathbf{J}_e \cdot \mathbf{n} \rangle$  is the projection of the total electronic angular momentum  $\mathbf{J}_e$  on the molecule-fixed internuclear axis  $\mathbf{n}$ ,  $\hat{z}$  is the laboratory-frame  $z$  axis defined by the direction of the external electric field,  $A_M$  and  $Z_M$  are the nucleon and the proton number of the heavy nucleus in the molecule  $M$ , respectively. The fit results are visualized in Fig. 1. Apart from the individual constraints from the paramagnetic systems ThO, HfF<sup>+</sup>, YbF, Tl, we show the one from Hg, as well as the combinations of only the paramagnetic constraints and the

Molecule	$\frac{E_{\text{eff}}}{(\text{GV/cm})}$	$\frac{W_S^{\text{a}}}{\text{kHz}}$	$\Omega$	$\langle \hat{n} \cdot \hat{z} \rangle$	$\frac{\alpha_{d_e}^M}{\text{mrad/s}/(10^{-27} e \text{ cm})}$	$\frac{\alpha_{C_S}^M}{10^7 \text{ mrad/s}}$	Refs.
HfF <sup>+</sup>	-23.0(0.9)	20.4(0.8)	1	1	$34.9 \pm 1.4$	$32.0 \pm 1.3$	[36, 45, 46]
ThO	-79.4(3.2)	112.1(4.5)	1	1	$120.6 \pm 4.9$	$181.6 \pm 7.3$	[24, 37, 38, 47]
YbF	23.1(1.8)	-40.5(3.2)	1/2	0.558	$-19.6 \pm 1.5$	$-17.6 \pm 2.0$	[39, 40, 48, 49]
Atom	$\alpha_{d_e}^A$	$\frac{\alpha_{C_S}^A}{10^{-20} e \text{ cm}}$					Refs.
Fr	$885 \pm 35$	$1090 \pm 17$					[50–52]
Tl	$-573 \pm 20^{\text{b}}$	$-700 \pm 35^{\text{c}}$					[56, 57]
Cs	$120 \pm 3$	$78 \pm 2$					[50, 55, 57, 58]
Rb	$25.7 \pm 0.8$	$11.0 \pm 0.2$					[50, 58]
Hg	$0.012 \pm 0.012$	$-0.028 \pm 0.006$					[59], this work

<sup>a</sup> Note the existence of different conventions in the literature; for instance, the coefficient  $W_S$  used here is called  $W_{T,P}$  in Ref. [45], while  $W_S$  in that reference denotes the product  $A/ZW_{T,P}$  appearing in Eq. (19).

<sup>b</sup> For discussions regarding this value, see also Refs. [53, 54]. Note that the global fit is not affected by this discussion.

<sup>c</sup> See also Ref. [55]

TABLE IV. Relevant information regarding the systems under consideration.  $\alpha_{d_e, C_S}^A$  are defined in analogy to Eq. (20) as  $d_A = \alpha_{d_e} d_e + \alpha_{C_S} C_S$ .

global fit to all systems. The fit to only paramagnetic systems is massively improved by the HfF<sup>+</sup> measurement: before this measurement it extended essentially over the whole green area. Our result for Mercury is seen to additionally improve the fit, reducing the model-independent limits for both quantities significantly. This is due to the constraint being essentially orthogonal to those from the paramagnetic systems: we obtain for the paramagnetic systems a range  $\alpha_{C_S}^{M,A}/\alpha_{d_e}^{M,A} \in [0.4, 1.5] \times 10^{-20} e \text{ cm}$ , while for Mercury we obtain conservatively  $\alpha_{C_S}^{\text{Hg}}/\alpha_{d_e}^{\text{Hg}} < -0.9 \times 10^{-20} e \text{ cm}$ . The latter ratio will be more precisely determined once the coefficient for the electron EDM in Hg is known better, which is work in progress; here we assumed an uncertainty of 100%, given the unreliable estimate. This improvement will also improve the determination of  $d_e$  and  $C_S$ . In Table V we give the numerical results of both fits (global and paramagnetic only), including the effective correlations between the results for  $d_e$  and  $C_S$ , as well as the corresponding upper limits. While the individual constraints from Hg are weaker than those extracted from ThO and HfF<sup>+</sup>, its inclusion in the global fit results in model-independent limits about a factor of two stronger than those from the paramagnetic systems alone.

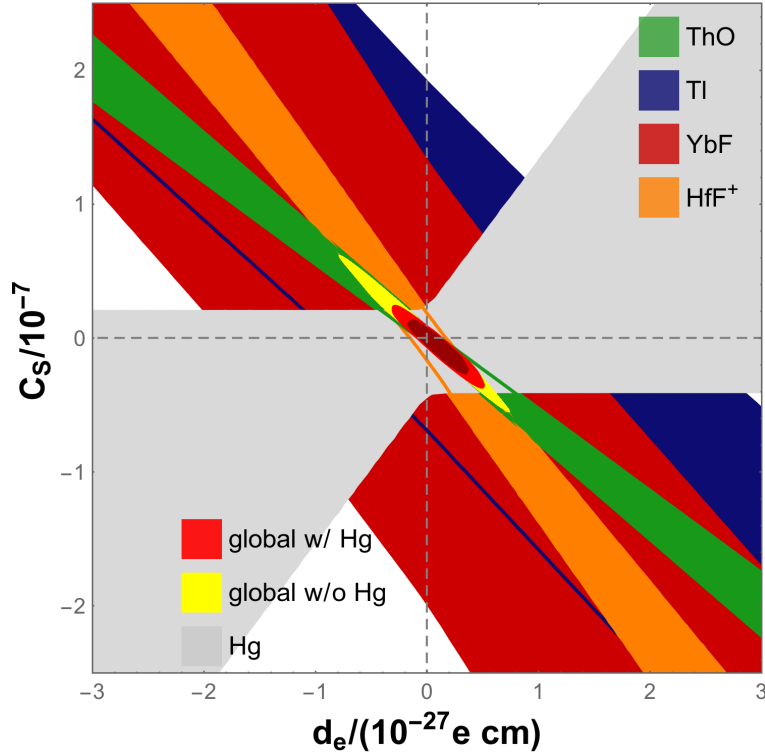


FIG. 1. Fit to the available data from paramagnetic systems plus the constraint from Mercury, using the result presented in this work. The bands from the individual constraints as well as the global fit without Mercury correspond to 95% CL, the global fit with Mercury to 68% and 95% CL. These bands include both experimental and theoretical uncertainties. Individual constraints have 1 effective degree of freedom, the global fits 2.

Fit	$d_e/10^{-28} e \text{ cm}$	$C_S/10^{-8}$	Correlation
global (w/ Hg)	$1.1 \pm 1.7$	$-0.6 \pm 1.2$	-96%
	$ d_e  \leq 3.8$	$ C_S  \leq 2.7$	
param. only (w/o Hg)	$-0.9 \pm 3.2$	$0.8 \pm 2.4$	-99%
	$ d_e  \leq 6.4$	$ C_S  \leq 4.9$	

TABLE V. Fit results for the global fit, using our result for Hg, and the fit using only the results from paramagnetic systems. The former yields limits about a factor of two stronger than the latter.

## V. CONCLUSIONS AND OUTLOOK

We performed global fits to the available data constraining the electron EDM and the S-PS-ne nucleon-electron coupling entering heavy atoms and molecules, using up-to-date calculations of the atomic and molecular structures. The inclusion of

the recent result on  $\text{HfF}^+$  ions improves drastically the fit to paramagnetic systems, only. As pointed out in Ref. [11], diamagnetic systems can be used to improve this fit additionally; while the corresponding contributions are heavily suppressed in this case, diamagnetic systems have the advantage of constraining in some cases combinations orthogonal to those accessible in paramagnetic systems. As an illustration we performed the first direct calculation of the coefficient of the S-PS-ne coupling in Mercury, including the effect of electron correlations. In combination with the recently improved experimental limit for this system we obtain limits on both the electron EDM and the S-PS-ne coupling of about a factor of two stronger than from paramagnetic systems alone, see Table V.

Having a model-independent determination of both quantities determining the EDMs of paramagnetic systems in hand, we proceed to evaluate the impact on ongoing searches. The global fits imply non-trivial upper limits for every paramagnetic system that is not effectively constraining the fits in Fig. 1. These limits, given in Table VI, indicate the necessary precision for a given system to contribute significantly to the global fit or the fit to paramagnetic systems, only (given in parentheses). A significant result above these limits would indicate an experimental problem. A measurement below the limit from the fit to paramagnetic systems, but above the one from the global fit, could in principle also indicate the contrived situation with a series of cancellations, described at the beginning section IV.

Atom	Limits for $ d_A /10^{-26}e\text{ cm}$	
	Inferred (this work)	Experimental
Rb	0.7 (1.2)	$10^8(1200)[60, 61]$
Cs	2.7 (4.2)	1400 [62]
Fr	13.0 (14.8)	—
Molecule	Limits for $ \omega_M /(\text{mrad/s})^*$	
YbF	3.7 (5.6)	27.8 [39, 40, 63]

TABLE VI. Model-independent limits for paramagnetic systems from our global fits; the numbers in brackets correspond to the fit including paramagnetic systems, only. \*: Assuming the same degree of polarization as in the previous experiment.

In the future, it is to be expected that measurements in paramagnetic systems alone will yield sufficiently precise results to limit or determine the two contributions discussed here by themselves. In that case our calculations will serve to improve the model-independent determination of hadronic contributions to diamagnetic EDMs in the context of a global fit extending over the whole set of P,T-odd interactions.

## VI. ACKNOWLEDGMENTS

This research was supported by the DFG cluster of excellence “Origin and Structure of the Universe”. The authors are grateful to the Mainz Institute for Theoretical Physics (mitp) for its hospitality and its partial support during the completion of this work.

- 
- [1] J. S. M. Ginges and V. V. Flambaum. Violations of fundamental symmetries in atoms and tests of unification theories of elementary particles. *Phys. Rev.*, 397:63, 2004.
  - [2] M. Pospelov and A. Ritz. Electric dipole moments as probes of new physics. *Ann. Phys.*, 318:119, 2005.
  - [3] M. Raidal et al. Flavour physics of leptons and dipole moments. *Eur. Phys. J.*, C57:13–182, 2008.
  - [4] T. Fukuyama. Searching for new physics beyond the standard model in electric dipole moment. *Int. J. Mod. Phys. A*, 27:1230015, 2012.
  - [5] J. Engel, M. J. Ramsey-Musolf, and U. van Kolck. Electric dipole moments of nucleons, nuclei, and atoms: The Standard Model and beyond. *Prog. Part. Nuc. Phys.*, 71:21, 2013.
  - [6] J. Bsaisou, Ulf-G. Meißner, A. Nogga, and A. Wirzba. P- and T-Violating Lagrangians in Chiral Effective Field Theory and Nuclear Electric Dipole Moments. *Annals Phys.*, 359:317–370, 2015.
  - [7] Timothy Chupp, Peter Fierlinger, Michael Ramsey-Musolf, and Jaideep Singh. Electric Dipole Moments of the Atoms, Molecules, Nuclei and Particles. 2017.
  - [8] M. Jung and A. Pich. Electric Dipole Moments in Two-Higgs-Doublet Models. *J. High Energy Phys.*, 4:076, 2014.
  - [9] B. Graner, Y. Chen, E. G. Lindahl, and B. R. Heckel. Reduced Limit on the Permanent Electric Dipole Moment of Hg199. *Phys. Rev. Lett.*, 116(16):161601, 2016. [Erratum: *Phys. Rev. Lett.*119,no.11,119901(2017)].
  - [10] V. A. Dzuba, V. V. Flambaum, and C. Harabati. Relations between matrix elements of different weak interactions and interpretation of the parity-nonconserving and electron electric-dipole-moment measurements in atoms and molecules. *Phys. Rev. A*, 84:052108, 2011. Erratum *ibid*, **85**, 029901 (2012).
  - [11] M. Jung. A robust limit for the electric dipole moment of the electron. *J. High Energy Phys.*, 5:168, 2013.
  - [12] L. I. Schiff. Measurability of Nuclear Electric Dipole Moments. *Phys. Rev.*, 132:2194, 1963.



- [13] I. B. Khriplovich and S. K. Lamoreaux. *CP Violation Without Strangeness*. Springer; Berlin, Heidelberg, 1997.
- [14] S. Knecht, H. J. Aa. Jensen, and T. Fleig. Large-Scale Parallel Configuration Interaction. II. Two- and four-component double-group general active space implementation with application to BiH. *J. Chem. Phys.*, 132:014108, 2010.
- [15] V. V. Flambaum and I. B. Khriplovich. New bounds on the electric dipole moment of the electron and on  $T$ -odd electron-nucleon coupling. *Sov. Phys. JETP*, 62:872, 1985.
- [16] T. Fleig and M. K. Nayak. Electron electric dipole moment and hyperfine interaction constants for ThO. *J. Mol. Spectrosc.*, 300:16, 2014.
- [17] M. Denis, M. Nørby, H. J. Aa. Jensen, A. S. P. Gomes, M. K. Nayak, S. Knecht, and T. Fleig. Theoretical study on  $\text{ThF}^+$ , a prospective system in search of time-reversal violation. *New J. Phys.*, 17:043005, 2015.
- [18] V. A. Dzuba, V. V. Flambaum, and S. G. Porsev. Calculations of the ( $P, T$ )-odd electric dipole moments for the diamagnetic atoms  $^{129}\text{Xe}$ ,  $^{171}\text{Yb}$ ,  $^{199}\text{Hg}$ ,  $^{211}\text{Rn}$ , and  $^{225}\text{Ra}$ . *Phys. Rev. A*, 80:032120, 2009.
- [19] N. J. Stone. *Table of nuclear magnetic dipole and electric quadrupole moments*. IAEA Nuclear Data Section Vienna International Centre, P.O. Box 100, 1400 Vienna, Austria, 2014. INDC International Nuclear Data Committee.
- [20] K. G. Dyall. Relativistic double-zeta, triple-zeta, and quadruple-zeta basis sets for the 5d elements Hf-Hg. *Theoret. Chim. Acta*, 112:403, 2004.
- [21] K. G. Dyall and A. S. P. Gomes. Revised relativistic basis sets for the 5d elements Hf-Hg. *Theoret. Chim. Acta*, 125:97, 2010.
- [22] A. Kramida, Yu. Ralchenko, J. Reader, and and NIST ASD Team. NIST Atomic Spectra Database (ver. 5.3), [Online]. Available: <http://physics.nist.gov/asd> [2017, February 21]. National Institute of Standards and Technology, Gaithersburg, MD., 2015.
- [23] L. Visscher and K. G. Dyall. *Atomic Data and Nuclear Data Tables*, 67:207, 1997.
- [24] M. Denis and T. Fleig. In search of discrete symmetry violations beyond the standard model: Thorium monoxide reloaded". *J. Chem. Phys.*, 145:028645, 2016.
- [25] T. Fleig, M. K. Nayak, and M. G. Kozlov. TaN, a molecular system for probing  $P, T$ -violating hadron physics. *Physical Review A*, 93:012505, 2016.
- [26] M. G. Kozlov. New Limit on the Scalar  $P, T$  Odd Electron Nucleus Interaction. *Phys. Lett.*, A130:426–428, 1988.
- [27] A. M. Mårtensson-Pendrill. Calculation of a  $P$ - and  $T$ -Nonconserving Weak Interaction in Xe and Hg with Many-Body Perturbation Theory. *Phys. Rev. Lett.*, 54:1153, 1985.

- [28] Laima Radžiūtė, Gediminas Gaigalas, Per Jönsson, and Jacek Bieroń. Electric dipole moments of superheavy elements - A case study on copernicium. *Phys. Rev.*, A93(6):062508, 2016.
- [29] K. V. P. Latha, D. Angom, B. P. Das, and D. Mukherjee. Probing CP violation with the electric dipole moment of atomic mercury. *Phys. Rev. Lett.*, 103:083001, 2009. [Erratum: *Phys. Rev. Lett.*115,no.5,059902(2015)].
- [30] N. Yamanaka, B. K. Sahoo, N. Yoshinaga, T. Sato, K. Asahi, and B. P. Das. Probing exotic phenomena at the interface of nuclear and particle physics with the electric dipole moments of diamagnetic atoms: A unique window to hadronic and semi-leptonic CP violation. *Eur. Phys. J.*, A53:54, 2017.
- [31] Yashpal Singh and B. K. Sahoo. Rigorous limits for hadronic and semi-leptonic  $CP$ -violating coupling constants from the electric dipole moment of  $^{199}\text{Hg}$ . *Phys. Rev.*, A91(3):030501, 2015.
- [32] B. K. Sahoo. Improved limits on the hadronic and semi-hadronic CP violating parameters and role of a dark force carrier in the electric dipole moment of  $^{199}\text{Hg}$ . 2016.
- [33] B. K. Sahoo and B. P. Das. Relativistic Normal Coupled-Cluster Theory for Accurate Determination of Electric Dipole Moments of Atoms: First application to  $^{199}\text{Hg}$  atom. *arXiv: 1801.07045*, 2018.
- [34] T. Chupp and M. Ramsey-Musolf. Electric dipole moments: A global analysis. *Phys. Rev. C*, 91:035502, 2015.
- [35] L. Visscher and K. G. Dyall. Dirac-Fock Atomic Electronic Structure Calculations using Different Nuclear Charge Distributions. *Atomic Data and Nuclear Data Tables*, 67:207, 1997.
- [36] William B. Cairncross, Daniel N. Gresh, Matt Grau, Kevin C. Cossel, Tanya S. Roussy, Yiqi Ni, Yan Zhou, Jun Ye, and Eric A. Cornell. Precision Measurement of the Electron’s Electric Dipole Moment Using Trapped Molecular Ions. *Phys. Rev. Lett.*, 119(15):153001, 2017.
- [37] The ACME Collaboration, J. Baron, W. C. Campbell, D. DeMille, J. M. Doyle, G. Gabrielse, Y. V. Gurevich, P. W. Hess, N. R. Hutzler, E. Kirilov, I. Kozyryev, B. R. O’Leary, C. D. Panda, M. F. Parsons, E. S. Petrik, B. Spaun, A. C. Vutha, and A. D. West. Order of Magnitude Smaller Limit on the Electric Dipole Moment of the Electron. *Science*, 343:269, 2014.
- [38] Jacob Baron et al. Methods, Analysis, and the Treatment of Systematic Errors for the Electron Electric Dipole Moment Search in Thorium Monoxide. *New J. Phys.*, 19(7):073029, 2017.
- [39] J. J. Hudson, D. M. Kara, I. J. Smallman, B. E. Sauer, M. R. Tarbutt, and E. A. Hinds. Improved measurement of the shape of the electron. *Nature*, 473:493, 2011.

- [40] D. M. Kara, I. J. Smallman, J. J. Hudson, B. E. Sauer, M. R. Tarbutt, and E. A. Hinds. Measurement of the electron’s electric dipole moment using YbF molecules: methods and data analysis. *New J. Phys.*, 14:103051, 2012.
- [41] B. C. Regan, E. D. Commins, C. J. Schmidt, and D. DeMille. New Limit on the Electron Electric Dipole Moment. *Phys. Rev. Lett.*, 88:071805, 2002.
- [42] P. G. H. Sandars. The electric dipole moment of an atom. *Phys. Lett.*, 14:194, 1965.
- [43] P. G. H. Sandars. Enhancement factor for the electric dipole moment of the valence electron in an alkali atom. *Physics Letters*, 22(3):290–291, 1966.
- [44] V.V Flambaum. On Enhancement of the electron Electric Dipole Moment in Heavy Atoms. *Yad.Fiz.*, 24:383–386, 1976.
- [45] L. V. Skripnikov. Communication: Theoretical study of HfF<sup>+</sup> cation to search for the T,P-odd interactions. *J. Chem. Phys.*, 147(2):021101, 2017.
- [46] T. Fleig. P,T -odd and magnetic hyperfine-interaction constants and excited-state lifetime for HfF<sup>+</sup>. *Phys. Rev. A*, 96(4):040502, 2017.
- [47] L. V. Skripnikov. Combined 4-component and relativistic pseudopotential study of ThO for the electron electric dipole moment search. *J. Chem. Phys.*, 145(21):214301, 2016.
- [48] M. Abe, G. Gopakumar, M. Hada, B. P. Das, H. Tatewaki, and D. Mukherjee. Application of relativistic coupled-cluster theory to the effective electric field in YbF. *Phys. Rev. A*, 90:022501, 2014.
- [49] A. Sunaga, M. Abe, M. Hada, and B. P. Das. Relativistic coupled-cluster calculation of the electron-nucleus scalar-pseudoscalar interaction constant  $W_S$  in YbF. *Phys. Rev. A*, 93:042507, 2016.
- [50] B. M. Roberts, V. A. Dzuba, and V. V. Flambaum. Double-core-polarization contribution to atomic parity-nonconservation and electric-dipole-moment calculations. *Phys. Rev. A*, 88(4):042507, 2013.
- [51] Debashis Mukherjee, B. K. Sahoo, H. S. Nataraj, and B. P. Das. Relativistic coupled cluster (rcc) computation of the electric dipole moment enhancement factor of francium due to the violation of time reversal symmetry . *The Journal of Physical Chemistry A*, 113(45):12549–12557, 2009.
- [52] L. V. Skripnikov, D. E. Maison, and N. S. Mosyagin. Scalar-pseudoscalar interaction in the francium atom. *Phys. Rev. A*, 95(2):022507, 2017.
- [53] H. S. Nataraj, B. K. Sahoo, B. P. Das, and D. Mukherjee. Reappraisal of the Electric Dipole Moment Enhancement Factor for Thallium. *Phys. Rev. Lett.*, 106:200403, 2011.
- [54] H. S. Nataraj, B. K. Sahoo, B. P. Das, and D. Mukherjee. Brief remarks on “Electric dipole moment enhancement factor of thallium”. *arXiv: 1202.5402*, 2012.

- [55] B K Sahoo, B P Das, R K Chaudhuri, D Mukherjee, and E P Venugopal. Atomic electric-dipole moments from Higgs-boson-mediated interactions. *Phys. Rev.*, A78:10501, 2008.
- [56] S. G. Porsev, M. S. Safronova, and M. G. Kozlov. Electric Dipole Moment Enhancement Factor of Tl. *Phys. Rev. Lett.*, 108:173001, 2012.
- [57] V. A. Dzuba and V. V. Flambaum. Calculation of the (T,P)-odd electric dipole moment of thallium and cesium. *Phys. Rev. A*, 80:062509, 2009.
- [58] H. S. Nataraj, B. K. Sahoo, B. P. Das, and D. Mukherjee. Intrinsic Electric Dipole Moments of Paramagnetic Atoms: Rubidium and Cesium. *Phys. Rev. Lett.*, 101:033002, 2008.
- [59] A. M. Mårtensson-Pendrill and P. Öster. Calculations of Atomic Electric Dipole Moments. *Phys. Scr.*, 36:444, 1987.
- [60] E. S. Ensberg. Experimental upper limit for the permanent electric dipole moment of  $\text{rb}^{85}$  by optical-pumping techniques. *Phys. Rev.*, 153:36–43, 1967.
- [61] F.R. Jr. Huang-Hellinger. *A Search for a Permanent Electric Dipole Moment in Rubidium*. PhD thesis, University of Washington, Seattle, 1987. Quoted in [13], unpublished.
- [62] S. A. Murthy, D. Krause, Z. L. Li, and L. R. Hunter. New Limits on the Electron Electric Dipole Moment from Cesium. *Phys. Rev. Lett.*, 63:965–968, 1989.
- [63] J. J. Hudson, B. E. Sauer, M. R. Tarbutt, and E. A. Hinds. Measurement of the Electron Electric Dipole Moment Using YbF Molecules. *Phys. Rev. Lett.*, 89:023003, 2002.